Materials Research Proceedings 41 (2024) 1807-1816 https://doi.org/10.21741/9781644903131-200

Influence of data filtering and noise on the calibration of constitutive models using machine learning techniques

PRATES Pedro[1,2,3,a*], PINTO José[4], MARQUES João[1], HENRIQUES João[1,2], PEREIRA André[3] and ANDRADE-CAMPOS António[1,2]

[1]Centre for Mechanical Technology and Automation (TEMA), Mechanical Engineering Department, University of Aveiro, Portugal

[2]Intelligent Systems Associate Laboratory (LASI), Portugal

[3]Centre for Mechanical Engineering, Materials and Processes (CEMMPRE), ARISE, Department of Mechanical Engineering, University of Coimbra, Coimbra, Portugal

[4]Physics Department, University of Aveiro, Portugal

[a]prates@ua.pt

Keywords: Parameter Identification, Machine Learning, Feature Analysis, Noise, Sheet Metal Forming

Abstract. This work focuses on predicting material parameters that describe the plastic behaviour of metallic sheets using the XGBoost machine learning algorithm, with a dual focus on the influence of data filtering and data noise. A dataset was populated with finite element simulation results of cruciform tensile tests, including strain field data during the test. Different noise levels were added to the strain-related features of the dataset; additionally, a feature importance study was carried out to identify and select the most relevant features of the dataset. A systematic analysis shows how feature noise and selection individually and simultaneously influence the predictive performance of machine learning models. The results show that feature selection will greatly accelerate model training, without losing its predictive performance. Also, adding noise to the features does not have significant impact on model performance, highlighting the robustness of the models.

Introduction

The essential role of numerical simulations in sheet metal forming processes for automotive and aerospace industries requires precise constitutive modeling. While existing strategies like Finite Element Model Updating (FEMU) and Virtual Fields Method (VFM) have been proposed, they present computational challenges [1, 2]. This study builds upon previous work by using machine learning, specifically the XGBoost algorithm, for material parameter identification. It extends prior work by employing machine learning, specifically the XGBoost algorithm, for material parameter identification. Initially, a dataset was generated using finite element simulation results from cruciform tensile tests. After preprocessing the dataset, the XGBoost algorithm was trained, and its performance in predicting material parameters was assessed. Subsequently, noise was introduced to the strain-related features to emulate scenarios like measurement-affecting errors in Digital Image Correlation (DIC), impacting computed strains via DIC. The performance of the model was re-evaluated under these conditions. Finally, a feature analysis was conducted to assess the robustness of machine learning models, considering only the most important features; the influence of added noise to the strain-related important features was again assessed.

Numerical simulation model

This study employs the biaxial tensile test on a cruciform sample as the chosen mechanical test. The sample's geometry, previously designed in a previous work [3], allows for the generation of

heterogeneous stress and strain fields, encompassing a diverse range of stress and strain paths commonly encountered in sheet metal forming processes. The cruciform sample's geometry and dimensions in the sheet plane are presented in Fig. 1(a). The numerical simulation model considers only one quarter of the sample, as indicated by the grey region in Fig. 1(a), due to symmetries in boundary conditions, sample geometry, and material behaviour. The simulation assumes plane stress conditions and maintains a constant thickness of the sheet. Fig. 1(b) depicts the boundary conditions and finite element mesh employed in the numerical model. Symmetry boundary conditions were applied on the 0x and 0y axes ($u_x = u_y = 0$ mm). Additionally, displacement boundary conditions are applied to nodes at the ends of both arms of the sample to ensure equal displacements along both 0x and 0y axes ($u_x = u_y = 2$ mm). The numerical model uses a regular mesh consisting of 405 CPS4R elements with bilinear shape functions and reduced integration. All finite element analysis (FEA) simulations are carried out using the ABAQUS CAE software [4]. Each simulation consists of twenty equally spaced time-steps, during which the forces along the 0x and 0y directions and the strain field (ε_x, ε_y, and ε_{xy}) are obtained at each time-step.

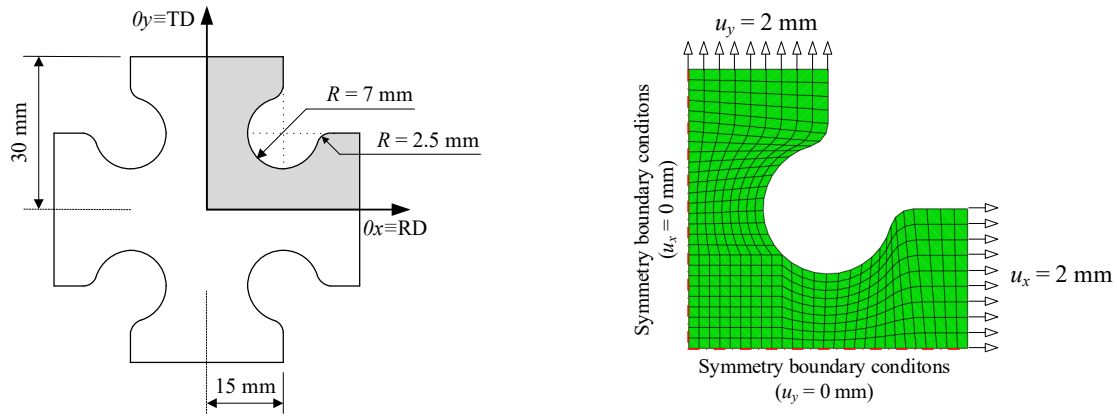

Fig. 1. Biaxial tensile test on a cruciform sample: (a) geometry and dimensions; (b) boundary conditions and finite element mesh.

The constitutive model of the material assumes an isotropic elastic behavior, described by the Hooke's law (with Young's modulus $E = 210$ GPa and Poisson's ratio $\nu = 0.3$), and an orthotropic plastic behavior, described by Hill'48 yield criterion with isotropic hardening described by Swift law under an associated flow rule. For plane stress conditions, the Hill'48 yield criterion can be written as follows:

$$(F+H)\sigma_{yy}^2 + (G+H)\sigma_{xx}^2 - 2H\sigma_{xx}\sigma_{yy} + 2N\tau_{xy}^2 = Y^2, \tag{1}$$

where F, G, H and N are anisotropy coefficients, σ_{xx}, σ_{yy} and τ_{xy} are the components of the Cauchy stress tensor in the material axes system of the metal sheet, and Y is the yield stress.
The condition $G+H=1$ (i.e. $\sigma_{xx} = Y$) was assumed, which corresponds to the following relationships:

$$F = \frac{r_0}{r_{90}(r_0+1)};\ G = \frac{1}{r_0+1};\ H = \frac{r_0}{r_0+1};\ N = \frac{1}{2}\frac{(r_0+r_{90})(2r_{45}+1)}{r_{90}(r_0+1)}, \tag{2}$$

where r_0, r_{45} and r_{90} are the Lankford coefficients obtained at 0º, 45º and 90º w.r.t. the rolling direction of the sheet, respectively. The Swift law describes the yield stress evolution during plastic deformation as follows:

$$Y = K\left[\left(\frac{\sigma_0}{K}\right)^{1/n} + \bar{\varepsilon}^{p}\right]^{n}, \quad (3)$$

where $\bar{\varepsilon}^{p}$ is the equivalent plastic strain and σ_0, K and n are material parameters.

Dataset generation, model training and performance evaluation

A total of 5733 sets of material parameters σ_0, K, n, r_0, r_{45} and r_{90} (i.e. samples) were generated using the Latin Hypercube Sampling (LHS) method. The input space the material parameters is: $\sigma_0 \in [120, 300]$ MPa, $K \in [280, 700]$ MPa, $n \in [0.10, 0.30]$; r_0, r_{45}, $r_{90} \in [0.600, 2.500]$. The step size for σ_0 and K is 1 MPa, for n is 0.01 and for r_0, r_{45} and r_{90} is 0.001. Numerical simulations of the cruciform tensile test were performed for each sample while maintaining the same geometry, boundary conditions and elastic properties. Fig. 2 presents an example of numerical results of the cruciform test that were used to build the dataset [2].

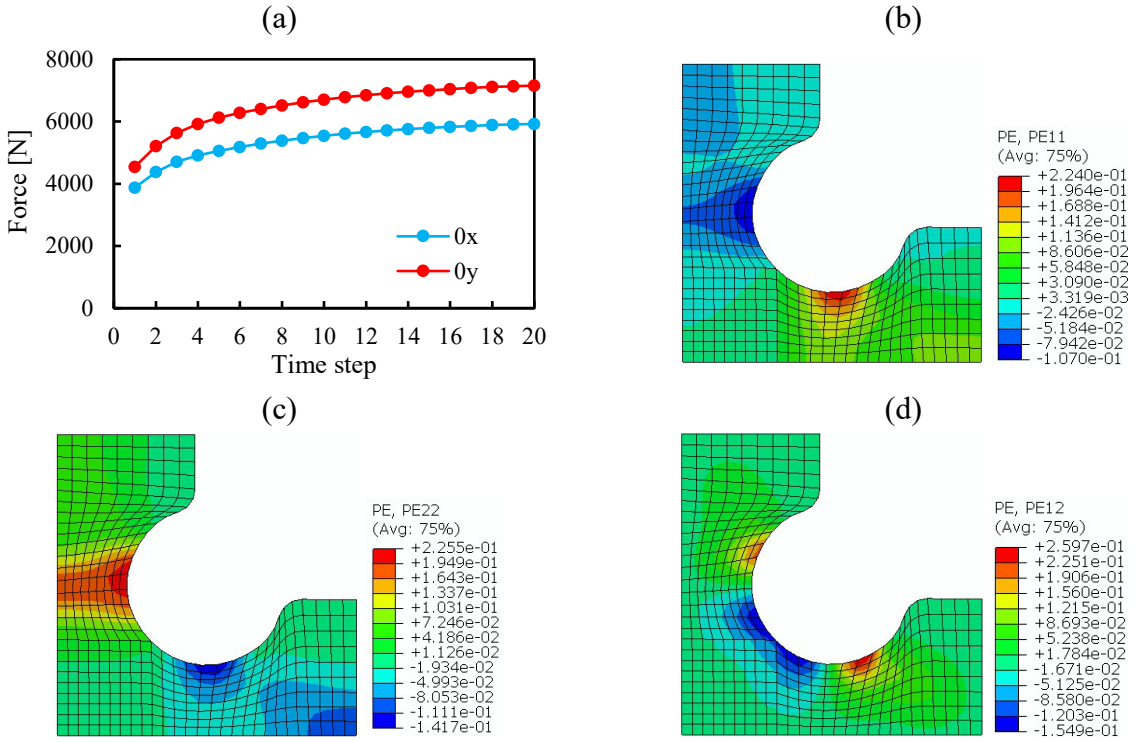

Fig. 2. FEA results of the cruciform test (Y_0=172MPa, n=0.16; K=486MPa; r_0=2.38; r_{45}=1.8; r_{90}=1.06) [2]: (a) load vs. displacement along the 0x and 0y axes; strain fields (b) ε_{xx}, (c) ε_{yy}, and (d) ε_{xy}. The strain fields (ε_{xx}, ε_{yy}, and ε_{xy}) were obtained for u_x=u_y=2mm.

Among the 5000 samples, 4671 exhibited no decrease in load during the simulation and were used for populating the dataset with synthetic data. Then, the dataset was randomly split into two subsets: a training set consisting of 4000 samples and a test set comprising 671 simulations. Each of the training and test sets consist of two matrices: a feature matrix and a target matrix. The feature matrix has shape $n_{samples} \times n_{features}$, where $n_{samples}$ is the total number of samples (i.e. numerical simulations) of the set and $n_{features}$ is the total number of features (20 timesteps×(2 forces + 3 strain components × 405 elements) = 24340). The target matrix has shape $n_{samples} \times n_{parameters}$, where $n_{outputs}$ is the total number of model outputs (i.e. material parameters). The feature and target matrices of the training set are shaped 4000×24340 and 4000×6, respectively, while the feature and target matrices of the test set have shape 671×24340 and 671×6, respectively. Fig. 3 shows the

distribution patterns of the material parameters for the 4671 samples. Distributions associated with parameter *n* exhibit constrained coverage in the input space, a result of a too large step size (0.01). Also, samples featuring combinations of high values of σ_0 and low values of *K* were excluded from the initial 5000 sets due to a observed decrease in load during the simulation; the same occurred for samples having σ_0 values inbetween 188 and 190 MPa (only 1 sample having 190MPa was not excluded).

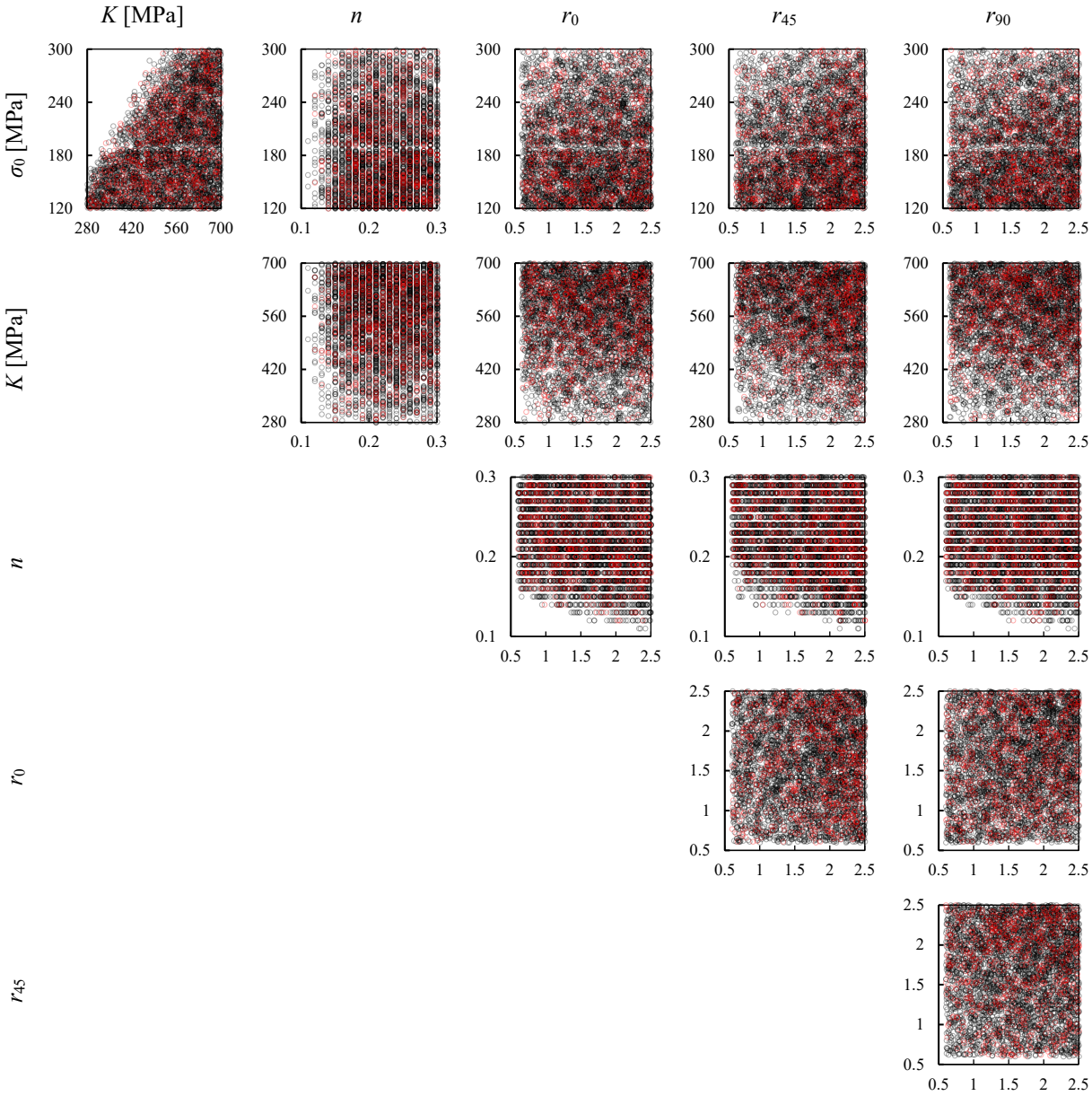

Fig. 3. Distribution patterns for material parameters in the training set (black markers) and test set (red markers).

The training set was used for training the Extreme Gradient Boosting (XGBoost) regression algorithm; more details regarding the XGBoost algorithm can be found in [1, 5]. The hyperparameters of the XGBoost regression algorithm were kept as default, except for the learning rate (=0.02), max_depth (=15) and n_estimators (=1000) [5]. The test set was used for evaluating the performance of the ML model in predicting the material parameters. Fig. 4 presents the performance evaluation of the ML model. It compares the σ_0, *n* and *K*, r_0, r_{45} and r_{90} values

predicted by the ML model with the real values considered in the FEA simulations of the test set. Generally, the machine learning model demonstrates superior predictive performance, as evidenced by the R^2 values presented in the figures.

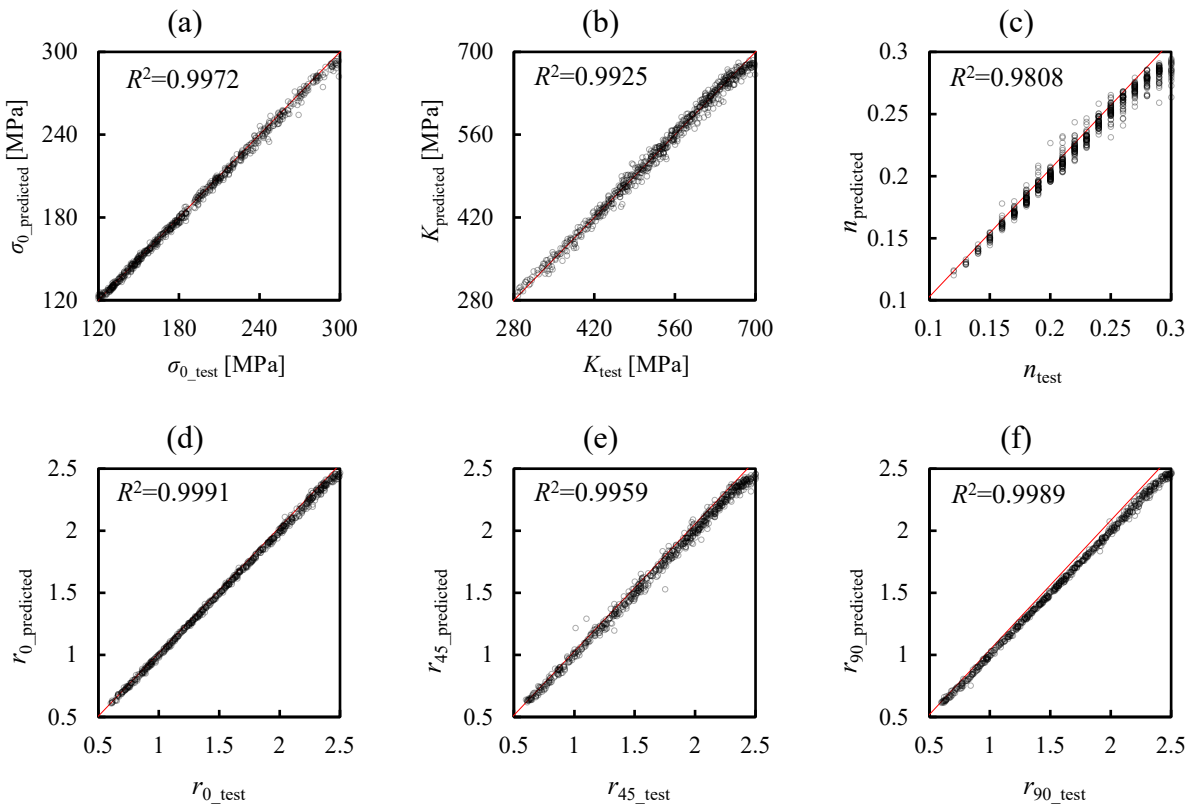

Fig. 4. Evaluation of constitutive parameter predictions for the test set: (a) σ_0; (b) K; (c) n; (d) r_0; (e) r_{45} and (f) r_{90}.

Performance evaluation with training set noise

Now, random noise following a uniform distribution is added to all strain-related features of the training dataset. This aims to replicate scenarios such as measurement-affecting errors in Digital Image Correlation (DIC) that influence the strains computed via DIC. Four distinct noise levels were taken into account (± 0%, ± 5%, ± 10%, ± 20%), with a model trained and evaluated for each level. Table 1 presents the R^2 values for the constitutive parameters under different noise ranges added to the training set. As noise levels increase, the model's adaptability and predictive performance are evaluated. Increasing the level of noise does not significantly diminish the model's performance in predicting the constitutive parameters. In fact, incorporating noise during training can enhance the robustness of the model and can contribute to a reduction in generalization error.

Table 1. Influence of added noise to the training set on model performance in predicting the material parameters.

Noise level	$R^2\_\sigma_0$	R^2_K	R^2_n	$R^2\_r_0$	$R^2\_r_{45}$	$R^2\_r_{90}$
± 0%	0.9972	0.9925	0.9808	0.9991	0.9959	0.9989
± 5%	0.9983	0.9917	0.9777	0.9992	0.9952	0.9991
± 10%	0.9983	0.9913	0.9771	0.9991	0.9951	0.9988
± 20%	0.9982	0.9908	0.9739	0.9981	0.9944	0.9980

An analysis of the overall relative error in predicting material parameters was carried out to assess the predictive performance of the models across the 671 simulations of the test set. This evaluation was performed using the Euclidean norm $\|\delta_j\|$, expressed as follows:

$$\|\delta_j\|(\%) = \sqrt{\frac{1}{m}\sum_{i=1}^{m}\left(\frac{x'_{i,j} - x_{i,j}}{x_{i,j}}\right)^2} \times 100\%\,,\ i=1,\ldots,m;\ j=1,\ldots 671, \tag{4}$$

where $x'_{i,j}$ and $x_{i,j}$ represent the estimated and true values of the i-th constitutive parameter in the j-th simulation in the testing set, and m is the total number of constitutive parameters to be identified (m=6). Fig. 5 presents $\|\delta_j\|$ as a function of the 671 simulations in the test set and compares the influence of noise added to the training set (± 0% *vs.* ± 20% added noise). In the case of the model trained on a noise-free training set, only 6 samples among the 671 exceed the 5% error threshold. However, for the model trained with ± 20% noise, only 11 samples exceed the 5% error threshold. These instances are minimal in comparison to the overall size of the test set, again highlighting the model's robustness in estimating material parameters even with added noise.

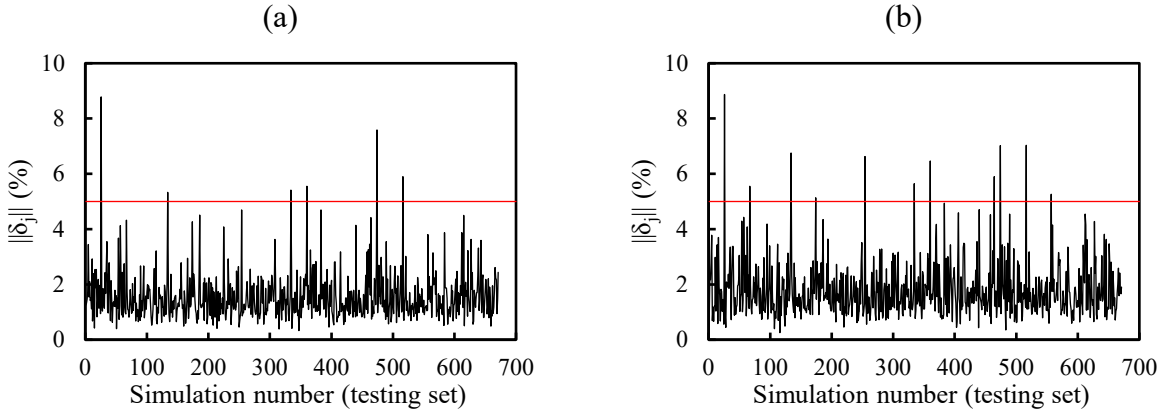

Fig. 5. Relative error $\|\delta_j\|$ in the prediction of material parameters for the 671 samples of the test set: (a) model trained with a noise-free training set; (b) model trained with ± 20% added noise.

Feature analysis and selection

As the previous ML models have demonstrated robustness to noise, a question arises: how does the sensitivity of the models to noise in the training set evolve when the dataset undergoes a substantial reduction in the number of features? To tackle this question, a features analysis using Shapley Additive Explanations (SHAP) is performed [6], to provide insights into the impact of employing a reduced dataset containing only the most influential features for the models to estimate the material parameters. Fig. 6 presents the 20 most influential features to predict each of the 6 material parameters. Each force feature is labelled as "Force_*direction*_*timestep*" (*direction* can be "x", or "y"; *timestep* ranges between 1 and 20), and each strain feature is labelled as "Strain_*component*_*elementnumber*_*timestep*" (*component* can be "x", "y", or "xy"; *elementnumber* ranges between 1 and 405 - see Fig. 1, and *timestep* ranges between 1 and 20). For example, according to Fig. 6 (a) and (b) the most influential features for predicting σ_0 and K are the force along the y direction at the first and last timesteps, respectively (which is naturally expected). For the trained model, an increase in the magnitudes of these features corresponds to an increase in the predicted values of the parameters, highlighting a positive correlation between these input features and the predicted outcomes. The remaining features shown in Fig. 6 (a) and

(b) are mostly strain-related features, which present little influence for predicting σ_0 and K. A similar analysis conducted for the remaining parameters reveals subtle insights that may not be immediately apparent. SHAP analysis contributes to a more comprehensive understanding of the relationships between the input features and the predicted outcomes for these material parameters.

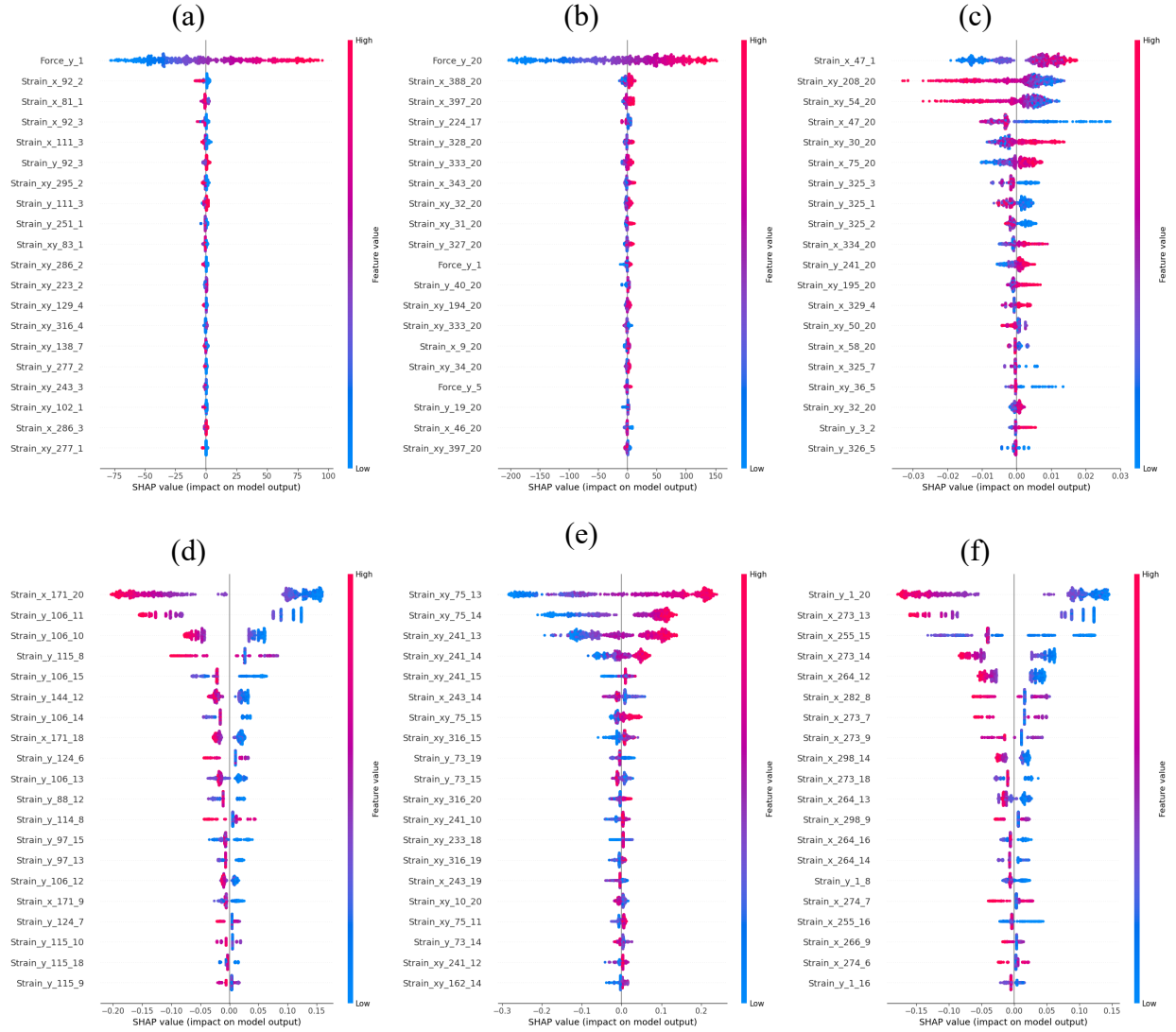

Fig. 6. SHAP feature importance analysis: (a) σ_0; (b) K; (c) n; (d) r_0; (e) r_{45} and (f) r_{90}.

Model noise sensitivity after feature selection

New training and test sets were generated by excluding features not displayed in Fig. 6 from the original training and testing sets. These refined new sets, each comprising 118 features (as opposed to the original 24340 features), served as the basis for further analysis. Additionally, a perturbed training set was derived from this refined training set, adding a noise level of ± 20% on the strain-related features. A model was trained with the refined training set, and another underwent training with the training set containing added noise. Both models achieved training completion in less than 1 minute, in contrast to the original training set, which required about 3 hours (13^{th} Gen Intel(R) Core(TM) i9-13900 24-core @2.00 GHz, 32 Gb RAM) . The validation of both models was conducted using the same training set. Table 2 presents the performance of the ML models trained with a refined training set, where the comparison focuses on models trained with a refined training set under two conditions: noise-free and with ± 20% added noise. The results show that the model only requires a small fraction of the original 243340 features to have excellent results in predicting

the values of the six material parameters. Incorporating a noise level of ± 20% results does not significantly diminish the model's predictive performance, as shown in Table 2. Comparing Fig. 7 to Fig. 5, only 6 samples exceed the 5% error threshold for the model trained with a noise-free set, and 11 samples for the model trained with ± 20% added noise. Again, these instances are minimal in comparison to the overall size of the test set, again demonstrating the model's robustness in estimating material parameters in the presence of added noise and assuming a small fraction of the total number of features.

Table 2. Influence of added noise to the refined training set on model performance in predicting the material parameters.

Noise range	$R^2\_\sigma_0$	R^2_K	R^2_n	$R^2\_r_0$	$R^2\_r_{45}$	$R^2\_r_{90}$
± 0%	0.9982	0.9935	0.9826	0.9991	0.9947	0.9991
± 20%	0.9981	0.9923	0.9688	0.9983	0.9934	0.9981

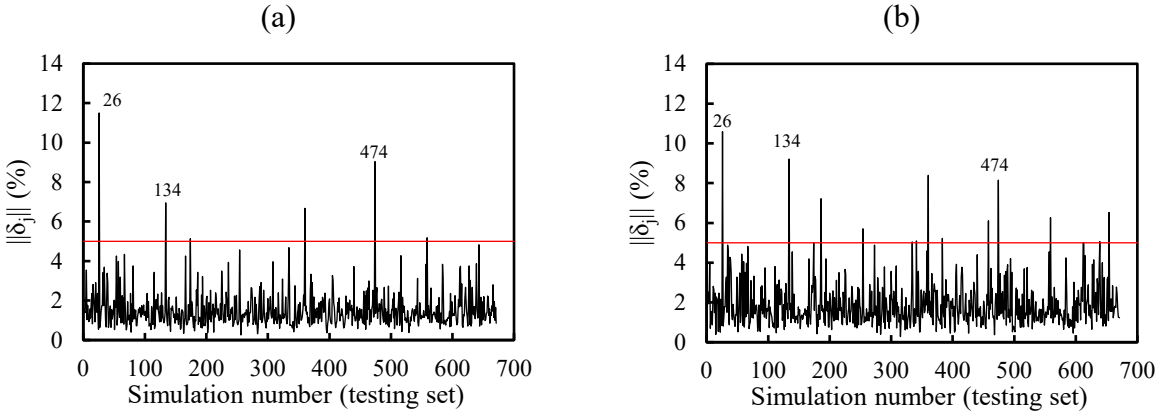

Fig. 7. Relative error $\|\delta_j\|$ in the prediction of material parameters for the 671 samples of the test set: (a) model trained with a noise-free training set; (b) model trained with ± 20% added noise. Models trained with only 118 features.

In Fig. 8, a comparison is presented between the actual and predicted hardening curves, along with Lankford coefficients in the sheet plane. This comparison focuses on 3 samples surpassing the 5% error threshold (see Fig. 7 (a)), considering the model trained with a noise-free dataset. Generally, the prediction error for the hardening curve remains below 2.5%. However, the maximum error in predicting the Lankford coefficients tends to exceed 5%, particularly at r_{45}, except for the sample labeled "134". This discrepancy may be attributed to the limited sensitivity of the cruciform test results in estimating r_{45}.

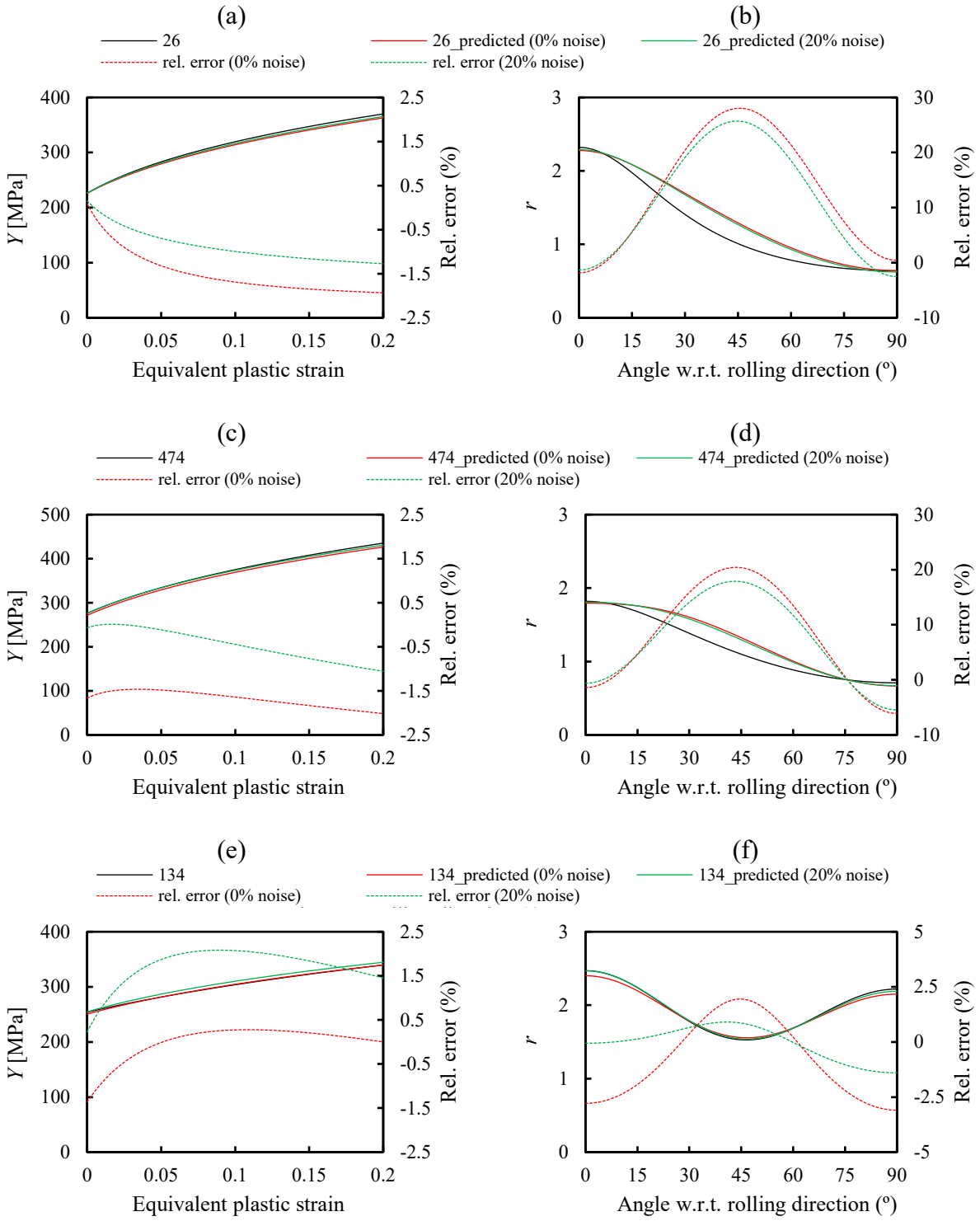

Fig. 8. Comparison between the actual and predicted hardening curves for samples labelled "26", "474" and "134", along with Lankford coefficients in the sheet plane.

Conclusions

This study demonstrates the effectiveness and competitiveness of machine learning-based techniques, namely using the XGBoost algorithm, in predicting material parameters for sheet metal forming simulations. Feature analysis highlights the significance of key features, accelerating model training without sacrificing predictive performance. The model's robustness is evident, with noise addition in key features minimally affecting predictive performance.

Acknowledgments
This work has received funding from the Research Fund for Coal and Steel under grant agreement No 888153. The authors also gratefully acknowledge the financial support of the Portuguese Foundation for Science and Technology (FCT) and by UE/FEDER through the programs CENTRO 2020 and COMPETE 2020, UIDB/00285/2020, UIDB/00481/2020 and UIDP/00481/2020-FCT, DOI 10.54499/UIDB/00481/2020 (https://doi.org/10.54499/UIDB/00481/2020) and DOI 10.54499/UIDP/00481/2020 (https://doi.org/10.54499/UIDP/00481/2020), CENTRO-01-0145-FEDER-022083, LA/P/0104/2020 and LA/P/0112/2020. It was also supported by the project RealForm (reference 2022.02370.PTDC), funded by Portuguese Foundation for Science and Technology. J. Henriques was supported by a grant for scientific research from the Portuguese Foundation for Science and Technology (ref. 2021.05692.BD).

References

[1] A. Andrade-Campos, N. Bastos, M. Conde, M. Gonçalves, J. Henriques, R. Lourenço, J.M.P. Martins, M.G. Oliveira, P. Prates, L. Rumor, On the inverse identification methods for forming plasticity models using full-field measurements, IOP Conf. Ser. Mater. Sci. Eng. 1238 (2022) 012059. https://doi.org/10.1088/1757-899X/1238/1/012059

[2] P.A. Prates, J.D. Henriques, J. Pinto, N. Bastos, A. Andrade-Campos, Coupling machine learning and synthetic image DIC-based techniques for the calibration of elastoplastic constitutive models, Mater. Res. Proc. 28 (2023) 1193-1202. https://doi.org/10.21741/9781644902479-130

[3] J. Martins, A. Andrade-Campos, and S. Thuillier, Calibration of anisotropic plasticity models using a biaxial test and the virtual fields method, Int. J. Solids Struct. 172 (2019) 21–37. https://doi.org/10.1016/j.ijsolstr.2019.05.019

[4] Dassault Systèmes. Abaqus 2017 documentation, 2017.

[5] T. Chen and C. Guestrin, XGBoost: A scalable tree boosting system, in Proceedings of the 22nd ACM SIGKDD International Conference on Knowledge Discovery and Data Mining (2016) 785–794. https://doi.org/10.1145/2939672.2939785

[6] S. Lundberg and S. Lee, “A Unified Approach to Interpreting Model Predictions”, 2017.